HHS Public Access

Author manuscript

*Shock*. Author manuscript; available in PMC 2021 July 01.

Published in final edited form as:

*Shock*. 2020 July ; 54(1): 96–101. doi:10.1097/SHK.0000000000001429.

# SIRT1 Mediates Septic Cardiomyopathy in a Murine Model of Polymicrobial Sepsis

**Lane M. Smith**[1], **Barbara K. Yoza**[1], **J. Jason Hoth**[1], **Charles E. McCall**[1], **Vidula Vachharajani**[2]

[1]Critical Illness, Injury and Recovery Research Center of Wake Forest School of Medicine, Winston Salem, NC 27157

[2]Department of Critical Care Medicine, Respiratory Institute, Cleveland Clinic Lerner College of Medicine, Cleveland, OH 44195

## Abstract

**BACKGROUND—**Cardiac dysfunction, a common complication from severe sepsis, is associated with increased morbidity and mortality. However, the molecular mechanisms of septic cardiac dysfunction are poorly understood. SIRT1, a member of the sirtuin family of NAD+-dependent protein deacetylases, is an important immunometabolic regulator of sepsis, and sustained SIRT1 elevation is associated with worse outcomes and organ dysfunction in severe sepsis. Herein, we explore the role of SIRT1 in septic cardiac dysfunction using a murine model of sepsis.

**METHODS—**An in vitro model of inflammation in isolated H9c2 cardiomyocytes was used to confirm SIRT1 response to stimulation with lipopolysaccharide (LPS), followed by a murine model of cecal ligation and puncture (CLP) to investigate the molecular and echocardiographic response to sepsis. A selective SIRT1 inhibitor, EX-527, was employed to test for SIRT1 participation in septic cardiac dysfunction.

**RESULTS—**SIRT1 mRNA and protein levels in cultured H9c2 cardiomyocytes were significantly elevated at later time points after stimulation with LPS. Similarly, cardiac tissue harvested from C57BL/6 mice 36 hours after CLP demonstrated increased expression of SIRT1 mRNA and protein compared to sham controls. Administration of EX-527 18 hours after CLP reduced SIRT1 protein expression in cardiac tissue at 36 hours. Moreover, treatment with EX-527 improved cardiac performance with increased global longitudinal strain and longitudinal strain rate.

**CONCULSIONS—**Our findings reveal that SIRT1 expression increases in isolated cardiomyocytes and cardiac tissue after sepsis-inflammation. Moreover, rebalancing SIRT1 excess in late sepsis improves cardiac performance suggesting that SIRT1 may serve as a therapeutic target for septic cardiomyopathy.

Please send all correspondence to Lane Smith, MD, PhD; Department of Emergency Medicine, Meads Hall 2nd Floor, Medical Center Blvd., Winston Salem, NC 27157.

## Introduction

Severe sepsis is a state of dysregulated inflammation and metabolism caused by infection that impairs organ function. It accounts for more than 700,000 emergency department visits and 200,000 deaths annually in the United States; the hospitalization rate from sepsis doubled in the past decade[1,2]. Cardiac performance in sepsis is typically hyperdynamic early in the disease, but often transitions to a stunned state characterized by impaired ventricular contractility, filling, cardiac index, and bioenergetics[3,4]. These reductions in ventricular function or elevations in cardiac biomarkers increase septic shock mortality up to 70% and suggests the heart is both an early marker of multi-organ dysfunction and a potential target for therapies to improve outcomes in severe sepsis[4,5]. Unfortunately, the molecular mechanisms of septic cardiac dysfunction are poorly understood.

Evidence suggests that SIRT1, a member of the sirtuin family of NAD+-dependent protein deacetylases, is an important regulator of cellular immunometabolism during sepsis[6,7]. SIRT1 expression in sepsis is characterized by an orderly transition from suppression in the hyperinflammatory acute phase, to excess in the hypoinflammatory adaptive phase, and finally a resolution to normal SIRT1 levels in homeostasis in surviving animals[6,7]. The mechanism of acute SIRT1 suppression is likely multifactorial with the availability of cofactor $NAD^+$ playing a key role; as $NAD^+$ accumulates in adaptive phase, SIRT1 activity and expression increases[7,8]. Persistent SIRT1 excess in adaptation is associated with organ dysfunction and likely contributes to septic cardiac dysfunction[8]. This premise is supported by studies linking the activation of Toll-like receptors (TLRs) to septic cardiac dysfunction through NF-κB activation[9]. TLR4 stimulation induces binding of SIRT1 and its cofactor $NAD^+$ to the promotor of inflammatory genes[10]. SIRT1 deactivates RelA/p65 through lysine 310 deacetylation and promotes termination of NF-κB-dependent transcription by deacetylating nucleosomal histone H4 lysine 16[10]. Although TLR4 is present on cardiomyocytes and NF-κB is activated by variety of disease states, there are no studies confirming SIRT1's role in cardiac dysfunction during adaptive sepsis[11].

Our study is the first linking cardiac stunning from sepsis to elevations in myocardial SIRT1 in late, adaptive sepsis. We show that cardiac SIRT1 is significantly increased at late time points in cultured myocytes after an inflammatory stimulus, and in cardiac tissue harvested from septic mice. Moreover, pharmacologic SIRT1 suppression in adaptation improves echocardiographic parameters of cardiac performance in sepsis.

## Methods

### Murine Sepsis

The described sepsis model was approved by the Institutional Animal Care and Use Committee of the Wake Forest University School of Medicine in accordance with National Institutes of Health guidelines. C57BL/6, 14- to 16-week-old male mice were obtained from The Jackson Laboratories (Bar Harbor, ME, USA), and the cecal ligation and puncture (CLP) procedure was performed under anesthesia as previously described[12]. Sham control mice underwent a similar procedure of cecal mobilization without ligation and puncture. The $LD_{50}$ of the CLP procedure is estimated at 77 hours after CLP.

## Cell Culture

H9c2 rat embryonal myoblast cells were obtained from American Type Culture Collection (ATCC; Manassas, VA, USA). The cells were grown in Dulbecco's modified Eagle's medium (DMEM, Thermo Fisher Scientific; Waltham, MA, USA ) with 10% heat-inactivated fetal bovine serum (FBS), penicillin (100 U/mL), streptomycin (100 mg/mL), at 37°C in 5% CO2 and 95% relative humidity. They were split 1:4 at subconfluence (80%) using a 0.25% Trypsin-EDTA solution (Thermo Fisher Scientific). Before each experiment, cells were seeded in six-well plates (Thermo Fisher Scientific Nunc) at the density of $5 \times 10^4$ cells/$cm^2$ and starved for 18 hours in DMEM containing 0.1% FBS. The cells were then treated with 1 μg/ml lipopolysaccharide (LPS; EMD Millipore/Sigma; Burlington, MA, USA) and harvested at 0 (untreated), 2, 4, 6, 12, and 24 hours. Alternatively, cells were pretreated with 1 μM EX-527 (Millipore/Sigma) for 1 hour prior to treatment with 1 μg/ml LPS, and harvested at 2 hours post-LPS treatment. Total RNA was extracted from H9c2 cells with TRIzol Reagent (Millipore/Sigma) according to the manufacturer's instructions. Protein was extracted with cold RIPA buffer supplemented with Halt Protease Inhibitor Cocktail (Thermo Fisher Scientific) by centrifugation at 14,000 g for 15 min at 4 °C.

## Echocardiography

Two-dimensional echocardiography was performed using a Vevo 2100 LAZR microultrasound system (FUJIFILM/VisualSonics, Inc.; Toronto, ON, Canada) equipped with a 30 MHz linear array transducer. Measurements were made at 36 hours after surgery on sham control mice, septic mice receiving DMSO vehicle, and septic mice receiving 10 mg/kg EX-527 (dissolved in DMSO; Millipore/Sigma) i.p. at 18 hours post-CLP[8]. M-mode images at the mid-papillary level in the parasternal short-axis along with 2-D mode images in the parasternal long and short axis views were obtained for conventional echocardiographic measurements. Images were recorded in a digital format on the device and analyzed to determine left ventricular ejection fraction (LVEF), left ventricular fractional shortening (FS), stroke volume (SV) and heart rate (HR) off-line by a single observer blinded to the treatments.

Strain echocardiography (SE) measurements were performed with speckle-tracking strain software (VevoStrain, FUJIFILM/VisualSonics Inc.)[13,14]. Images acquired in the parasternal long axis view of the heart were used to measure global longitudinal strain (GLS) and peak longitudinal strain rate (LSR). Images acquired in the parasternal short axis view were used to measure global circumferential strain (GCS) and peak circumferential strain rate (CSR). Off-line SE analysis was accomplished by manual contouring of the endocardial and epicardial borders by a single blinded observer. Images were analyzed using the speckle-tracking software using frame-to-frame movement of discrete patterns of echoes (i.e. "speckles") present in myocardium and integrated over five cardiac cycles. Strain representing the difference between the final length of each segment relative to its resting length [(L1−L0)/L0] was calculated with more negative values indicating better systolic function.

### Cardiac Tissue Harvest

Mice were sacrificed and their hearts removed and weighed. The aorta was cannulated and retro-perfused with PBS to remove excess blood. The tissue was homogenized with mortar and pestle followed by protein extraction with 1.5 ml T-PER Extraction Reagent with Halt Protease Inhibitor Cocktail (10μl/ml; Thermo Fisher Scientific).

### Immunohistochemistry

Sections of heart from mice were harvested 36 hours after CLP or sham surgery, fixed in 10% formalin, paraffin embedded, and stained using SIRT1 antibodies (Santa Cruz Biotechnology, Inc. Dallas, TX, USA) and Cy™ 3-conjugated labeled secondary antibodies (Jackson Immuno Research Laboratories, Inc. West Grove, PA, USA).

### mRNA Analysis

Levels of SIRT1 and TNFα μRNA were determined by quantitative real-time RT-PCR using gene-specific TaqMan primer and probe sets (Thermo Fisher) using GAPDH mRNA as the internal loading control. Measures were made in an ABI prism 7000 sequence detection system (Applied Biosystems/Thermo Fisher Scientific).

### Western Blot Analysis

Protein concentration was measured on the digested supernatant from cardiac digests or H9c2 cells using a Pierce BCA Protein Assay Kit (Thermo Fisher Scientific). Equal amounts (50 μg) of protein were separated by SDS-PAGE electrophoresis and transferred to a polyvinylidene difluoride membrane (Thermo Fisher Scientific). Blots were blocked with 5% milk-TBS for 1 hour at room temperature and probed overnight at 4 °C with primary antibodies against SIRT1 (1:1000 dilution; Millipore/Sigma). β-actin served as a loading control and was probed with β-actin monoclonal antibody (Millipore/Sigma). SIRT1 and β-actin proteins were detected by incubation for 1 hour at room temperature with secondary antibody (Millipore/Sigma) diluted at 1:5000 in blocking buffer and then measured using a Li-Cor Odyssey Infrared Imaging System (Li-Cor Biosciences, Lincoln, NE, USA).

### Statistical Analysis

Data is presented as mean + SD unless otherwise noted. Single comparisons between two independent means were made using Student t test. One-way analysis of variance was performed on multiple comparisons of means using the Prism GraphPad data analysis software (GraphPad Software Inc., La Jolla, CA) followed by post-hoc comparison of multiple means via Tukey's Honest Range Test or Sidak's Multiple Comparison Test. Significant differences were determined at the $P < 0.05$ level.

## Results

### Inflammation Increases SIRT1 in Cardiomyocytes

To determine a role for SIRT1 during cardiac inflammation, cardiomyocytes were stimulated with LPS and SIRT1 mRNA and protein levels were measured at various times after LPS. Figure 1A shows that SIRT1 mRNA levels transiently decreased and then significantly

increased during LPS treatment. A corresponding increase in SIRT1 protein levels was also observed (Figures 1B and C). To establish a role for SIRT1 in regulating NF-κB dependent cardiac inflammation, TNFα mRNA levels in LPS treated myocytes were also measured. Figure 1 D shows that early LPS stimulation increased TNFα mRNA that was further increased by SIRT1 inhibition via EX-527 pretreatment at 2 hours. These results confirm a role for SIRT1 in regulating cardiac inflammation and support that SIRT1 may mediate septic cardiac dysfunction.

### Sepsis-Induced Cardiac Dysfunction Is Reversed by SIRT1 Inhibition

To determine a role for SIRT1 in septic cardiac dysfunction, adult mice were randomized to sham surgery, CLP, and CLP plus EX-527 after 18-hours and echocardiographic parameters were measure 36 hours after surgery. Baseline LVEF and HR were measured and similar between the cohorts. Table 1 shows there was no change in HR among the cohorts at 36 hours after surgery. LVEF determined by M-mode analysis was significantly decreased in the CLP treated mice when compared to sham treated at 36 hours post-surgery and did not increase with EX-527 treatment. SV significantly decreased in CLP treated mice at 36 hours largely due to a significant decrease in left ventricular end-diastolic volume (LVEDV) since left ventricular end-systolic volume (LVESV) remained relatively constant. However, the SV was significantly greater in EX-527 treated mice compared to CLP alone that was likely due to combined improvements in LVEDV and LVESV. Speckle-tracking strain analysis performed on the three cohorts showed significant decreases (i.e. less negative) in GLS and LSR at 36 hours post-CLP compared to sham treated mice. GLS and LSR values significantly improved with EX-527 treatment at 18 hours indicating a recovery in cardiac function due to SIRT1 inhibition. There was no difference in GCS and CSR between sham, CLP, and CLP plus EX-527 cohorts at 36 hours.

### SIRT1 in Cardiac Tissue Increases in Adaptive Sepsis

Whole hearts were harvested at 12 or 36 hours after sham, CLP, or CLP plus EX-527 to test the effect of sepsis on SIRT1 expression in cardiac tissue. A separate cohort of control mice that received no surgery was also harvested. Figures 2A and B show no difference in cardiac tissue SIRT1 steady state mRNA or protein across all cohorts measured at 12 hours. However, the CLP cohort demonstrated higher levels of SIRT1 mRNA and protein at 36 hours compared to the control and sham cohorts. Treatment with EX-527 at 18 hours decreased SIRT1 protein but not mRNA toward baseline levels at 36 hours. Cardiac tissue samples that underwent immunohistochemical staining of SIRT1 in septic mice 36 hours after surgery with and without treatment with 10 mg/kg EX-527 18 hours after surgery showed that SIRT1 staining (bright red) in septic mice was decreased by the administration of EX-527 (Figures 3A, B, and C).

## Discussion

This study shows increased cardiac SIRT1 expression during septic cardiomyopathy in adaptive sepsis. We demonstrate late increases in SIRT1 expression in both isolated cardiomyocyte models of inflammation using cultured H9c2 cardiomyocytes as well as a whole-organ model of infection using cardiac tissue digest. This increase in SIRT1

corresponds to impaired echocardiographic performance in adaptive sepsis. In addition, our data supports the hypothesis that rebalancing the increased SIRT1 expression in adaptive sepsis with the specific SIRT1 inhibitor EX-527 improves echocardiographic parameters of cardiac performance.

Previous studies in isolated immune cells describe a biphasic distribution of SIRT1 in sepsis with acute SIRT1 suppression that transitions to increased SIRT1 expression in adaptive sepsis and rebalancing to normal SIRT1 levels if the organism is to survive[6,7]. This biphasic distribution of SIRT1 expression corresponds to acute hyperinflammation followed by a late period of immune suppression when SIRT1 is overexpressed. Timing of this transition, which occurs between 18–24 hours after an infectious insult, has therapeutic implications since early pharmacologic SIRT1 suppression worsens outcomes in septic mice while late inhibition improves survival[8]. Although acute SIRT1 suppression was previously seen in a study of cardiac tissue harvested from septic mice harvested eight hours after CLP, this study did not investigate later time points[15]. Thus, our findings in both cultured cardiomyocytes and harvested tissue are the first evidence that cardiac SIRT1 expression exhibits a biphasic response across the acute and adaptive sepsis continuum. Moreover, the fact that SIRT1 excess is present in both cultured cardiomyocytes and harvested tissue provides an important proof of concept that SIRT1 elevations in whole-organ models are derived directly from cardiomyocytes, and not local inflammatory cells or connective tissue.

Of note, treatment with EX-527 at 18 hours reduces SIRT1 protein expression but not mRNA transcription suggesting a post-translational mechanism for SIRT1 inhibition. This is consistent with previous studies of EX-527's post-translational mechanism of binding to the nicotinamide site, preventing SIRT1's catalytic activity, and rendering the molecule susceptible to degradation by phosphorylation, oxidation by reactive oxygen species, nitrosylation, ubiquitination, and glutathionylation[16–18]. The fact that EX-527 primarily inhibits SIRT1 activity might explain why we did not see dramatic reductions in SIRT1 expression after treatment on immunohistochemistry analysis.

Previous studies of cardiac performance in sepsis using only conventional M-mode echocardiographic measurements of systolic function such as LVEF and FS were inconsistent due to dependence on preload and afterload conditions that are highly variable due to vasoplegia and capillary leak that is associated with sepsis[19,20]. SE measurements of myocardial contractility provide a more reliable assessment of cardiac performance than conventional LVEF in sepsis where cardiac loading conditions are variable[21,22]. While our measurements of LVEF and FS are likely confounded by significant variations in cardiac loading conditions, our SE analysis of cardiac performance is consistent with previous studies using SE at similar time points after CLP[23]. Moreover, our finding that late SIRT1 inhibition improves both GLS and LSR in septic mice suggests improved cardiac performance that is independent of loading conditions and directly relates to improved myocardial contractility. Thus, we show a physiologic basis for previous observations that late SIRT1 inhibition with EX-527 improves survival in septic mice[8].

Limitations from this focused analysis SIRT1 in septic cardiomyopathy largely relate to our narrow time course. We did not evaluate the effect of EX-527 on cardiac dysfunction later

than 36 hours post-sepsis since mortality from the CLP procedure significantly increases after 48 hours. In addition, we did not quantify cardiac SIRT1 expression in the first 12 hours of sepsis when SIRT1 is expected to be suppressed, nor did we test the effect of early SIRT1 activation (i.e. resveratrol) on early cardiac performance. Furthermore, the exact post-translational modification of SIRT1 in cardiac tissue and/or isolated cardiomyocytes needs further elucidation in future work.

In summary, our study supports the hypothesis that increased SIRT1 expression in the late, adaptive phase of sepsis is associated with cardiac dysfunction. Moreover, rebalancing late SIRT1 excess in the heart with the SIRT1 inhibitor EX-527 improves SE measurements of cardiac performance. Future studies are needed to determine if these changes in cardiac SIRT1 expression during sepsis are associated with alterations in myocardial metabolism since SIRT1 serves as both an immunologic and metabolic rheostat. Other avenues for investigation will focus on the interplay of septic cardiac dysfunction with chronic oxidative stress caused by smoking, obesity, and other long-term modulators of SIRT1 activity. Once finished, we hope to determine a role for SIRT1 and other sirtuins as therapeutic targets in sepsis or other acute illnesses.

## ACKNOWLEDGMENTS

This work was supported by the following U.S. National Institutes of Health grant R01GM099807.

The authors thank Dr. Leanne Groban (Wake Forest School of Medicine, Winston-Salem, NC, USA) for providing the H9c2 cardiomyocytes used in this study.

## References

1. Dombrovskiy VY, Martin AA, Sunderram J, Paz HL. Rapid increase in hospitalization and mortality rates for severe sepsis in the United States: A trend analysis from 1993 to 2003. Crit Care Med; 35(5): 1244–1250, 2007. [PubMed: 17414736]
2. Angus DC, Linde-Zwirble WT, Lidicker J, Clermont G, Carcillo J, Pinsky MR. Epidemiology of severe sepsis in the United States: Analysis of incidence, outcome, and associated costs of care. Crit Care Med; 29(7): 1303–1310, 2001. [PubMed: 11445675]
3. Zaky A, Deem S, Bendjelid K, Treggiari MM. Characterization of cardiac dysfunction in sepsis: an ongoing challenge. Shock; 41(1): 12–24, 2014. [PubMed: 24351526]
4. Landesberg G, Gilon D, Meroz Y, Georgieva M, Levin PD, Goodman S, Avidan A, Beeri R, Weissman C, Jaffe AS, et al. Diastolic dysfunction and mortality in severe sepsis and septic shock. Eur Heart J; 33(7): 895–903, 2012. [PubMed: 21911341]
5. Landesberg G, Jaffe AS, Gilon D, Levin PD, Goodman S, Abu-Baih A, Beeri R, Weissman C, Sprung CL, Landesberg A. Troponin elevation in severe sepsis and septic shock: the role of left ventricular diastolic dysfunction and right ventricular dilatation. Crit Care Med; 42(4): 790–800, 2014. [PubMed: 24365861]
6. McCall CE, Yoza B, Liu T, El Gazzar M. Gene-specific epigenetic regulation in serious infections with systemic inflammation. J Innate Immun; 2(5): 395–405, 2010. [PubMed: 20733328]
7. Liu TF, Brown CM, El Gazzar M, McPhail L, Millet P, Rao A, Vachharajani VT, Yoza BK, McCall CE. Fueling the flame: bioenergy couples metabolism and inflammation. J Leukoc Biol; 92(3): 499–507, 2012. [PubMed: 22571857]
8. Vachharajani VT, Liu T, Brown CM, Wang X, Buechler NL, Wells JD, Yoza BK, McCall CE. SIRT1 inhibition during the hypoinflammatory phenotype of sepsis enhances immunity and improves outcome. J Leukoc Biol; 96(5): 785–96, 2014. [PubMed: 25001863]

9. Gao M, Wang X, Zhang X, Ha T, Ma H, Liu L, Kalbfleisch JH, Gao X, Kao RL, Williams DL, Li C. Attenuation of Cardiac Dysfunction in Polymicrobial Sepsis by MicroRNA-146a Is Mediated via Targeting of IRAK1 and TRAF6 Expression. J Immunol; 195(2): 672–82, 2015. [PubMed: 26048146]
10. Liu TF, Yoza BK, El Gazzar M, Vachharajani VT, McCall CE. NAD+-dependent SIRT1 deacetylase participates in epigenetic reprogramming during endotoxin tolerance. J Biol Chem; 286(11): 9856–64, 2011. [PubMed: 21245135]
11. Knowlton AA. Paying for the Tolls: The High Cost of the Innate Immune System for the Cardiac Myocyte. Adv Exp Med Biol; 1003: 17–34, 2017. [PubMed: 28667552]
12. Hubbard WJ, Choudhry M, Schwacha MG, Kerby JD, Rue LW 3rd, Bland KI, Chaudry IH. Cecal ligation and puncture. Shock; 24: Suppl 1:52–7, 2005. [PubMed: 16374373]
13. Langeland S, Wouters PF, Claus P, Leather HA, Bijnens B, Sutherland GR, Rademakers FE, D'hooge J. Experimental assessment of a new research tool for the estimation of two-dimensional myocardial strain. Ultrasound Med Biol; 32(10): 1509–13, 2006. [PubMed: 17045871]
14. Haileselassie B, Su E, Pozios I, Niño DF, Liu H, Lu DY, Ventoulis I, Fulton WB, Sodhi CP, Hackam D, et al. Myocardial oxidative stress correlates with left ventricular dysfunction on strain echocardiography in a rodent model of sepsis. Intensive Care Med Exp; 5(1): 21. doi:10.1186/s40635-017-0134-5, 2017. [PubMed: 28405943]
15. Zheng Zhibo, Ma He, Zhang Xia, Tu F, Wang X, Ha T, Fan M, Liu L, Xu J, Yu K et al. Enhanced glycolytic metabolism contributes to cardiac dysfunction in polymicrobial sepsis. J Infect Dis; 215(9): 1396–1406, 2017. [PubMed: 28368517]
16. Gertz M, Fischer F, Nguyen GT, Lakshminarasimhan M, Schutkowski M, Weyand M, Steegborn C. Ex-527 inhibits Sirtuins by exploiting their unique NAD+-dependent deacetylation mechanism. Proc Natl Acad Sci U S A; 110(30): E2772–81, 2013. [PubMed: 23840057]
17. Gao Z, Zhang J, Kheterpal I, Kennedy N, Davis RJ, Ye J. Sirtuin 1 (SIRT1) protein degradation in response to persistent c-Jun N-terminal kinase 1 (JNK1) activation contributes to hepatic steatosis in obesity. J Biol Chem; 286(25): 22227–22234, 2011. [PubMed: 21540183]
18. Zhao X, Jin Y, Yang L, Hou Z, Liu Y, Sun T, Pei J, Li J, Yao C, Wang X, et al. Promotion of SIRT1 protein degradation and lower SIRT1 gene expression via reactive oxygen species is involved in Sb-induced apoptosis in BEAS-2b cells. Toxicol Lett; 296: 73–81, 2018. [PubMed: 30055241]
19. Huang SJ, Nalos M, McLean AS. Is early ventricular dysfunction or dilatation associated with lower mortality rate in adult severe sepsis and septic shock? A meta-analysis. Crit Care; 17(3): R96, 2013. [PubMed: 23706109]
20. Werdan K, Oelke A, Hettwer S, Nuding S, Bubel S, Hoke R, Russ M, Lautenschläger C, Mueller-Werdan U, Ebelt H. Septic cardiomyopathy: hemodynamic quantification, occurrence, and prognostic implications. Clin Res Cardiol; 100(8): 661–8, 2011. [PubMed: 21308379]
21. Vignon P, Huang SJ. Global longitudinal strain in septic cardiomyopathy: the hidden part of the iceberg? Intensive Care Med; 41(10): 1851–3, 2015. [PubMed: 26183488]
22. Sanfilippo F, Corredor C, Fletcher N, Tritapepe L, Lorini FL, Arcadipane A, Vieillard-Baron A, Cecconi M. Left ventricular systolic function evaluated by strain echocardiography and relationship with mortality in patients with severe sepsis or septic shock: a systematic review and meta-analysis. Crit Care; 22(1): 183, 2018. [PubMed: 30075792]
23. Haileselassie B, Su E, Pozios I, Niño DF, Liu H, Lu DY, Ventoulis I, Fulton WB, Sodhi CP, Hackam D, et al. Myocardial oxidative stress correlates with left ventricular dysfunction on strain echocardiography in a rodent model of sepsis. Intensive Care Med Exp; 5(1): 21, 2017. [PubMed: 28405943]

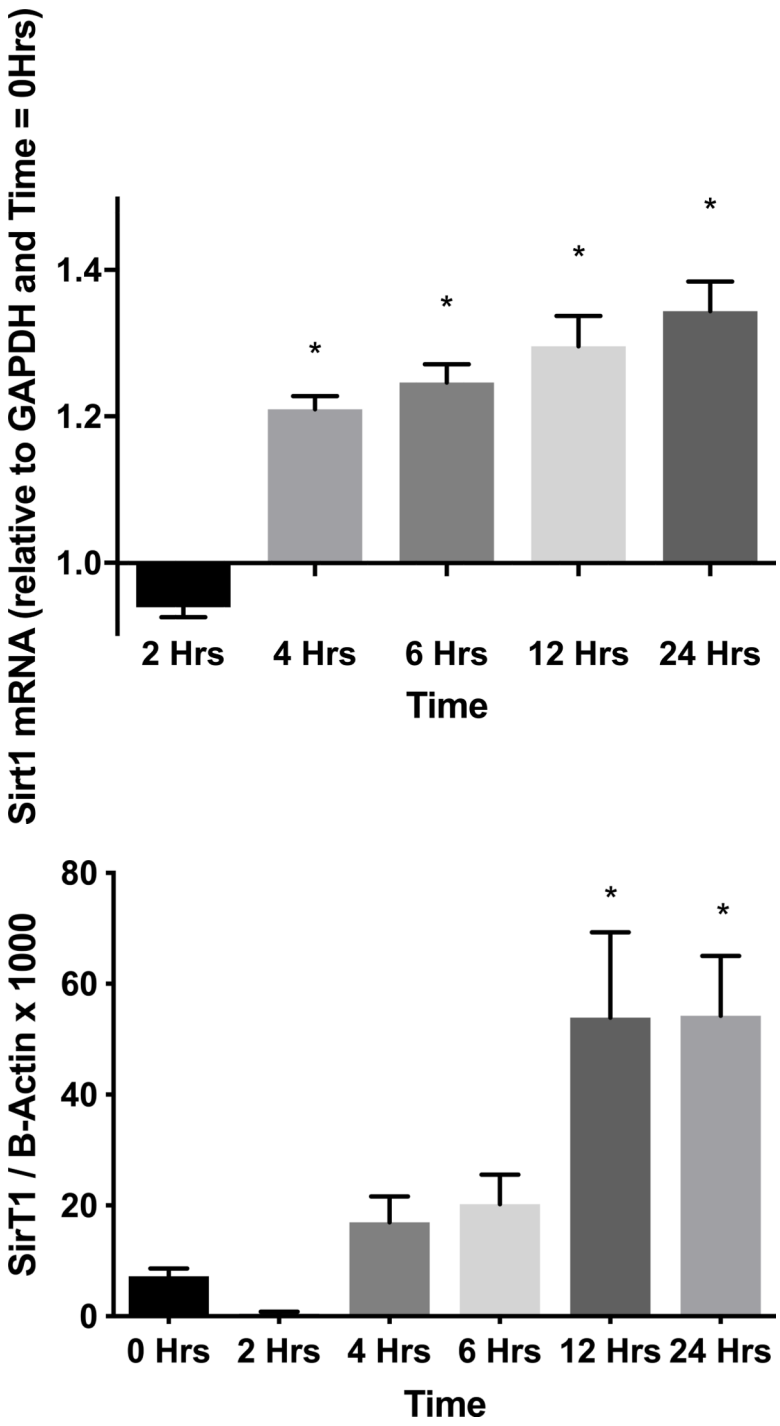

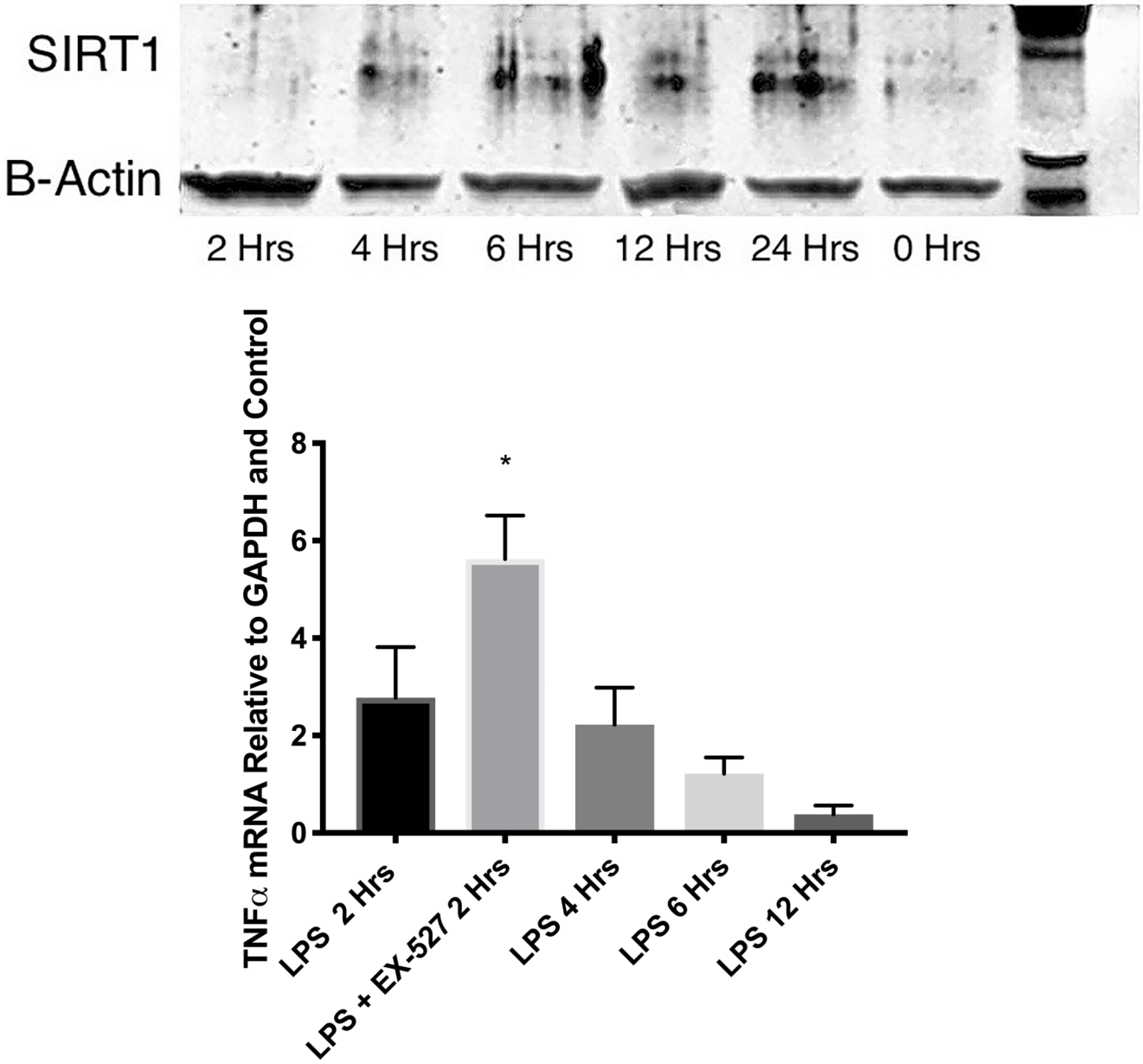


**Figure 1.**

(A)SIRT1 mRNA by RT-PCR in cultured H9c2 cardiomyocytes (n=5) relative to GAPDH and baseline (time 0) at 2, 4, 6, 12, and 24 hours after treatment with 1 μg/ml LPS. * Indicates significant increases in SIRT1 mRNA were noted at 4, 6, 12, and 24 hours ($p<0.001$) when compared to 2 hours. (B and C) SIRT1 protein relative to β-actin by Western Blot in cultured H9c2 cardiomyocytes (n=5) treated with 1 μg/ml LPS at 0, 2, 4, 6, 12, and 24 hours. * Indicates significant ($p<0.01$) increases in SIRT1 protein relative to time=0 noted at 12 and 24 hours. (D) TNFα mRNA relative to GAPDH and control by RT-PCR 2 hours after treatment with 1 μg/ml LPS was significantly increased by a 1-hour pretreatment with the SIRT1 inhibitor EX-527 ($p<0.01$).

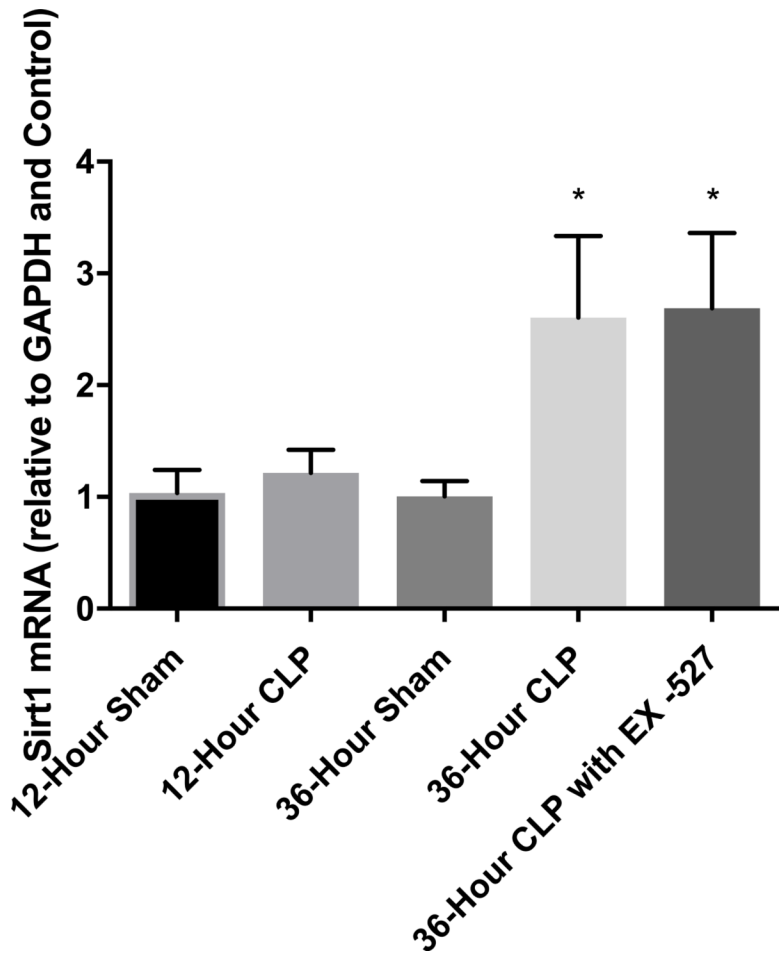

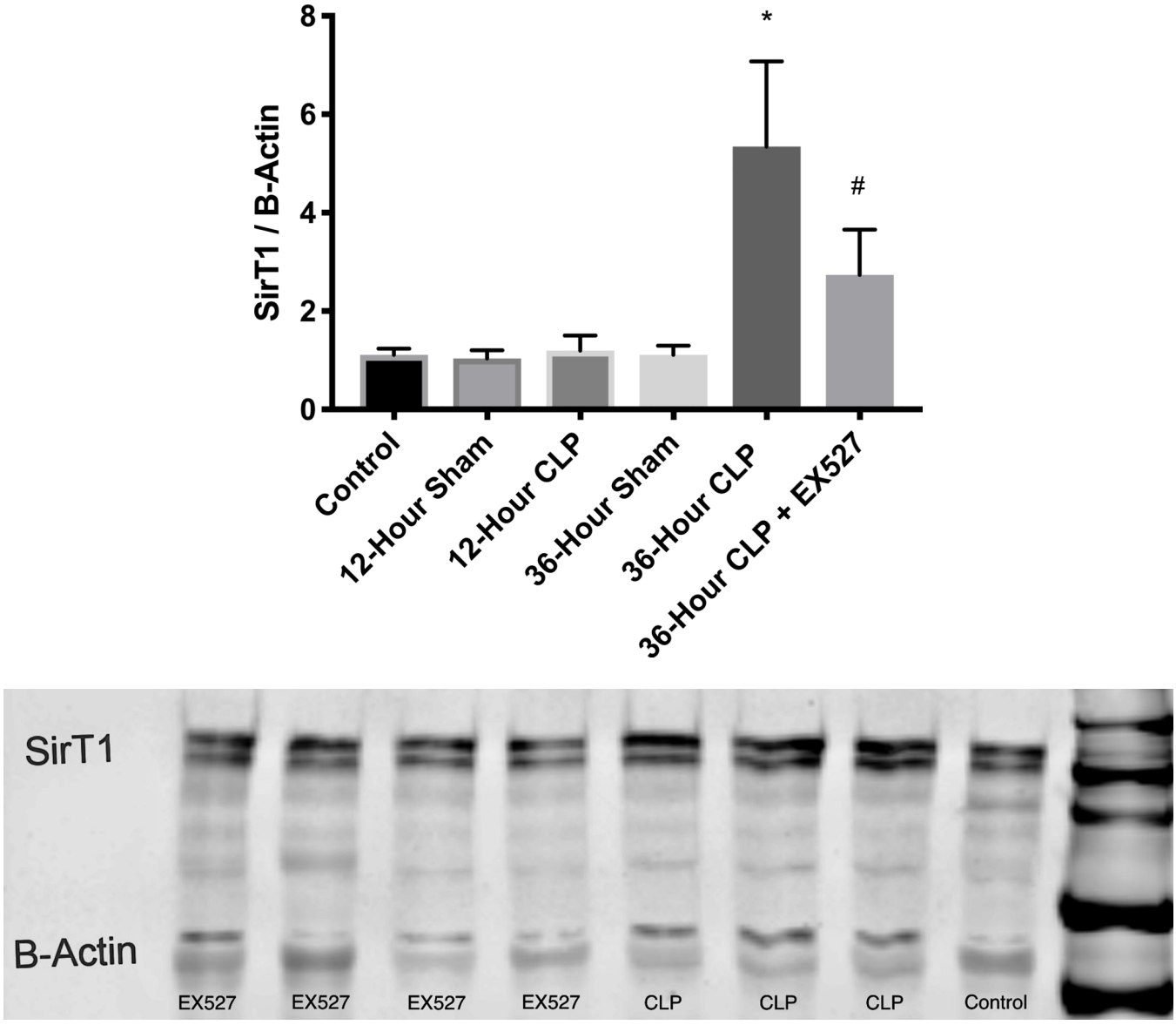


**Figure 2.**

Cardiac tissue harvest for SIRT1 mRNA and protein in control (n=3), 12-hour sham (n=8), 12-hour CLP (n=8), 36-hour sham (n=8), 36-hour CLP (n=8), and 36-hour CLP + 10mg/kg EX-527 at 18 hours post CLP (n=6). (A) SIRT1 mRNA relative to GAPDH and control by RT-PCR in cardiac tissue. * Indicates significant ($p<0.001$) increases in SIRT1 mRNA were noted at 36 hours in animals receiving CLP and CLP + EX-527 relative to animals receiving sham surgery or CLP at earlier time points. (B) SIRT1 protein relative to β-actin by Western Blot in control. * Indicates a significant increase ($P<0.001$) in SIRT1 protein at 36 hours in animals receiving CLP compared to all earlier time points. Administration of EX-527 significantly decreased ($p<0.01$) SIRT1 protein compared to CLP alone at 36 hours as indicated by #. (C) Sample Western Blot of control, CLP at 36 hours, and CLP+EX-527 at 36 hours.

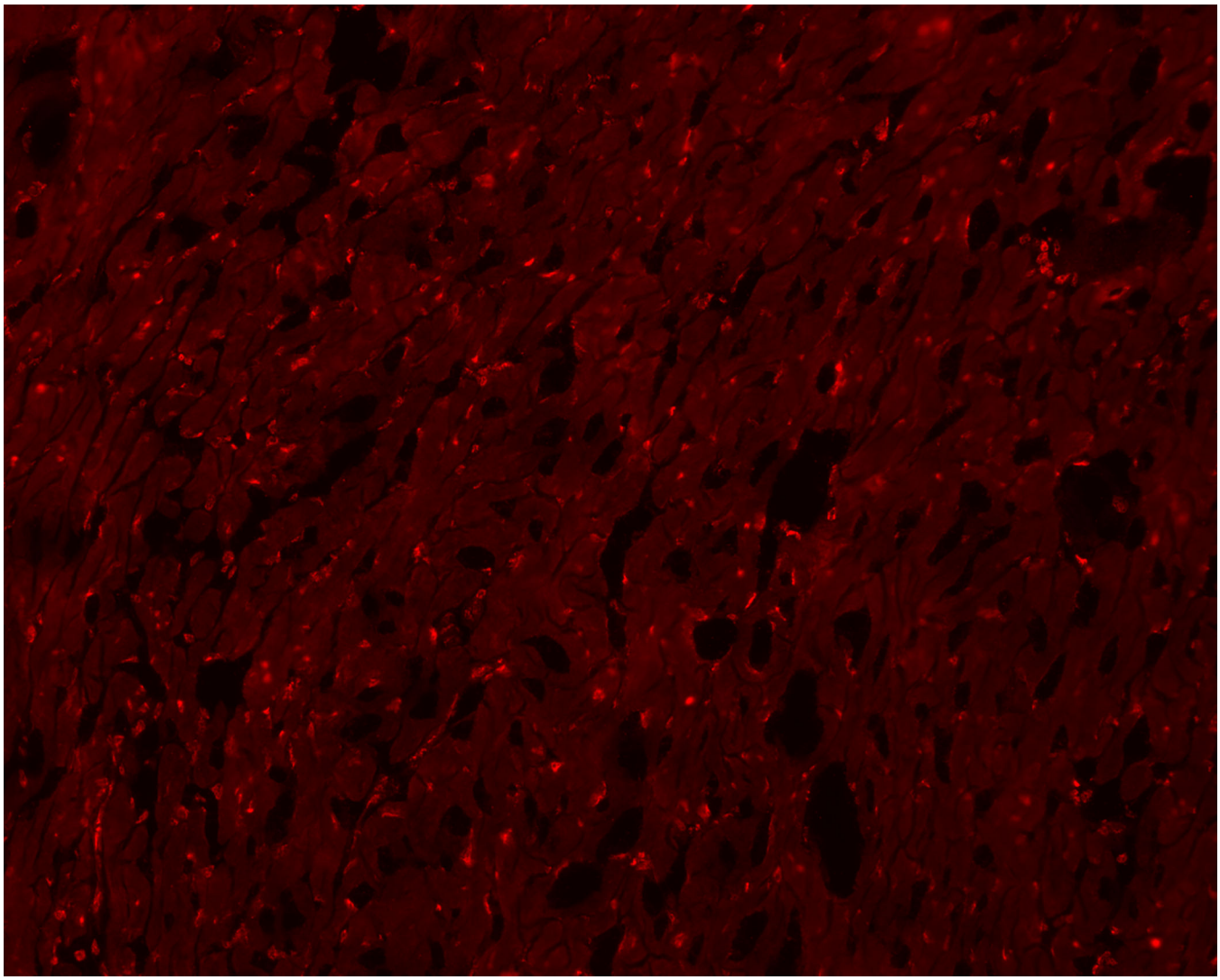

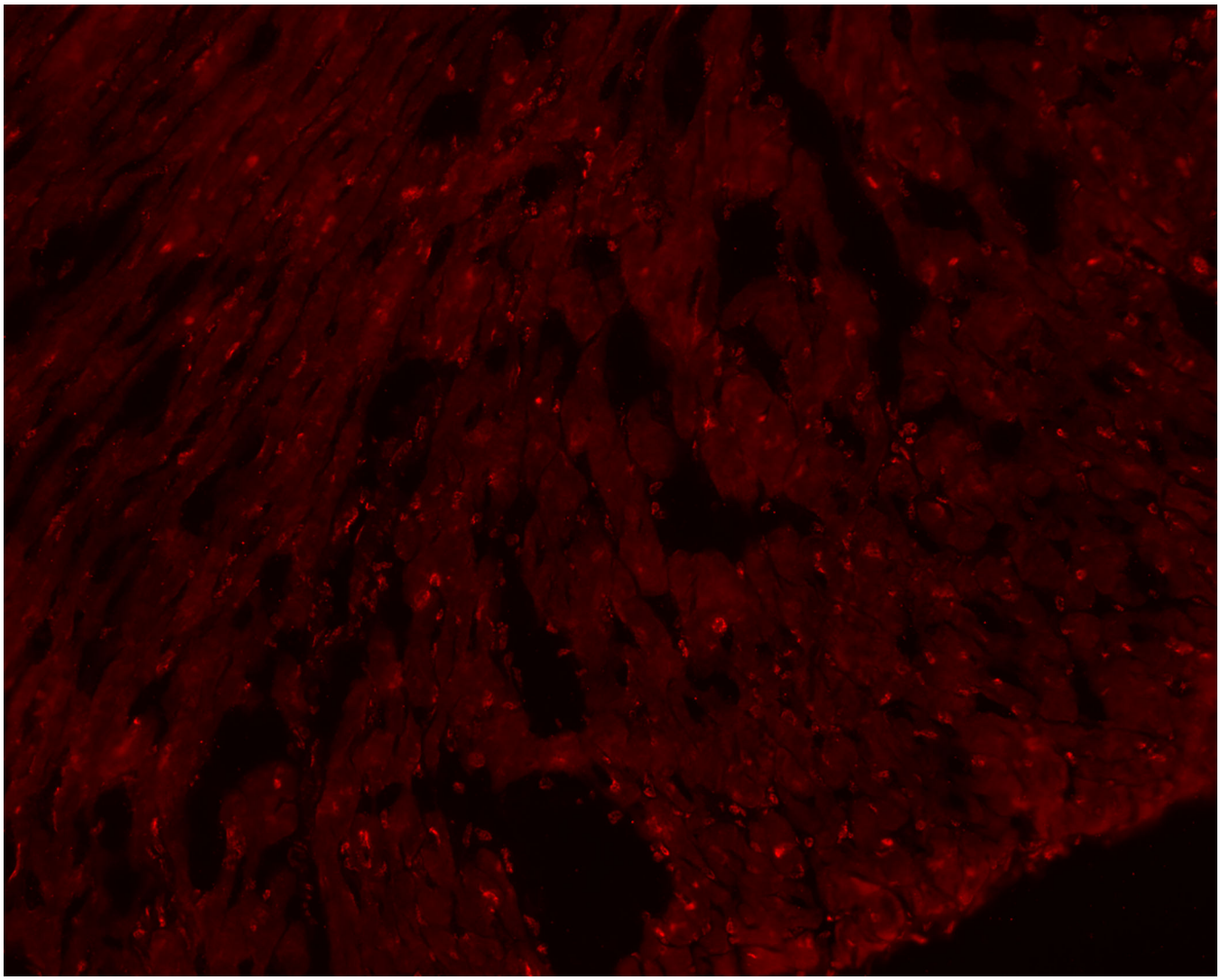

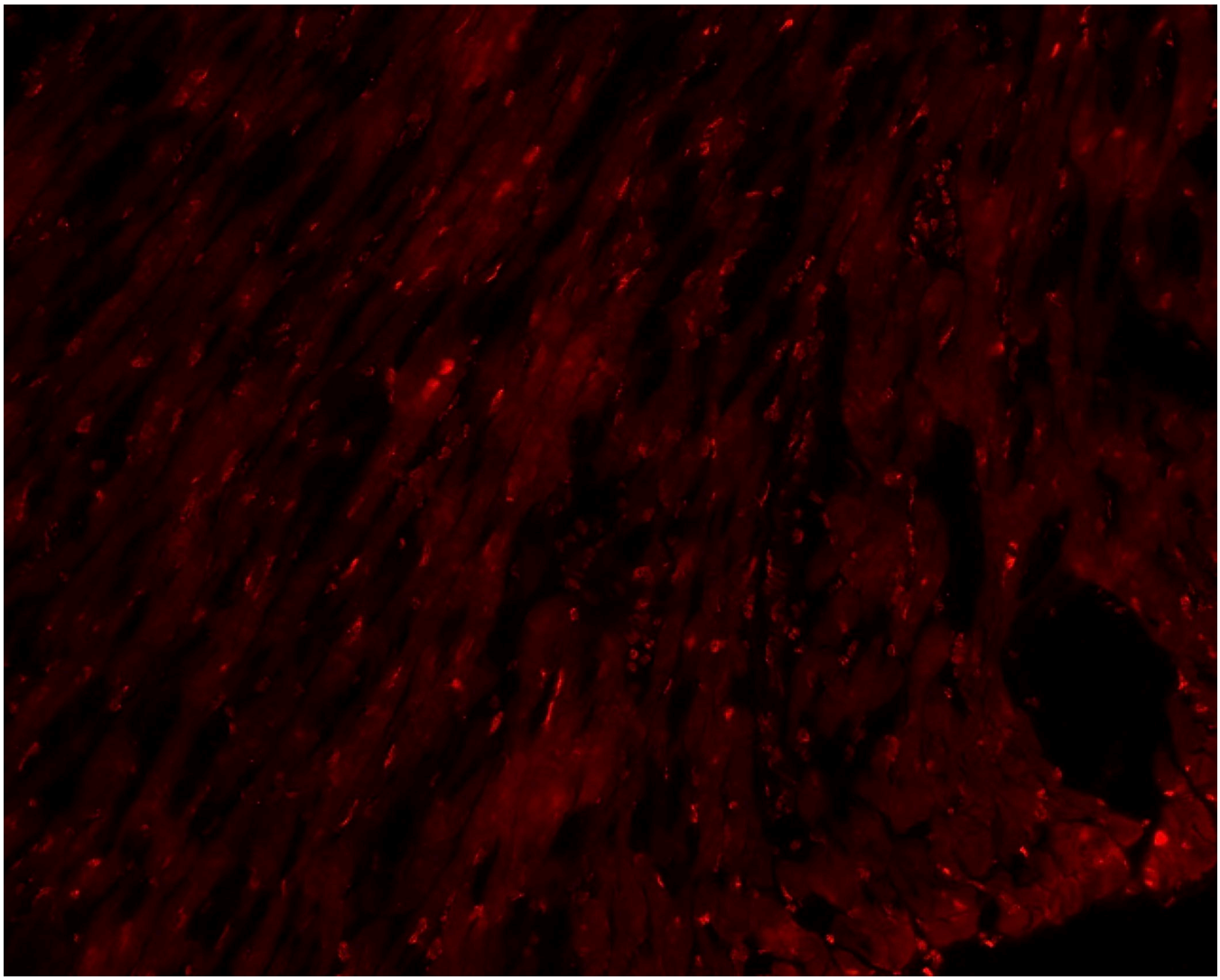

**Figure 3.**

36-hours after CLP, cardiac tissue was removed from septic mice (A) and compared to heart tissue from septic mice treated with EX-527 at 18 hours post-CLP (B) and sham treated mice (C). Higher intensity red staining in panel A indicates higher levels of SIRT1 expression in the myocardium of septic animals relative to sham or those treated with EX-527.

**Table 1.**

Echocardiographic parameters 36 hours after surgery using M-mode and strain analysis 36 hours after surgery. *CLP* indicates cecal ligation and puncture, *CLP + EX* mice treated with EX-527 18 hours after surgery, *SV* stroke volume, *LVEDV* left ventricular end-diastolic volume, LVESV left ventricular end-systolic volume, LVEF left ventricular ejection fraction, *FS* left ventricular fractional shortening, *GLS* global longitudinal strain, *LSR* peak longitudinal strain rate, *GCS* global circumferential strain, and *CSR* peak circumferential strain rate.

| Variable | Control (8) | CLP (8) | CLP + EX (8) | Significance |
|---|---|---|---|---|
| Mass (g) | 24.7 ± 2.0 | 25.5 ± 2.2 | 25.9 ± 1.9 | p = 0.55 |
| Heart Rate (bpm) | 461 ± 33 | 415 ± 64 | 430 ± 104 | p = 0.39 |
| M-Mode Analysis | | | | |
| SV (μL) | 43 ± 7 | 26 ± 3 * | 34 ± 6 # | p < 0.02 |
| LVEDV (μL) | 55 ± 9 | 42 ± 9 * | 50 ± 8 | p < 0.03 |
| LVESV (μL) | 12 ± 4 | 16 ± 7 | 16 ± 5 | p = 0.25 |
| LVEF (%) | 75 ± 7 | 62 ± 12 * | 61 ± 9 | p < 0.02 |
| FS (%) | 47 ± 4 | 33 ± 8 * | 33 ± 7 | p < 0.005 |
| Strain Analysis | | | | |
| GLS (%) | −24.34 ± 3.49 | −14.44 ± 2.99 * | −21.45 ± 3.63 # | p < 0.01 |
| LSR (%) | −10.16 ± 2.62 | −4.84 ± 2.00 * | −9.88 ± 3.93 # | p < 0.01 |
| GCS (%) | −29.23 ± 4.6 | −22.76 ± 5.43 | −29.45 ± 5.84 | p = 0.06 |
| CSR (%) | −10.75 ± 3.28 | −9.99 ± 3.84 | −11.00 ± 5.34 | p = 0.93 |

* Indicates significant difference between CLP and control

# indicates significant difference between CLP and CLP + EX cohorts.